Defect modes in one-dimensional comblike photonic waveguides

J. O. Vasseur,* B. Djafari-Rouhani, L. Dobrzynski, and A. Akjouj

*Laboratoire de Dynamique et Structures des Matériaux Moléculaires, UPRESA CNRS 8024, UFR de Physique,
Université de Lille I, 59655 Villeneuve d'Ascq Cédex, France*

J. Zemmouri

*Laboratoire de Physique des Lasers, Atomes et Molécules, Centre d'Etudes et de Recherches Lasers et Applications,
UMR CNRS 8523, Université de Lille I, 59655 Villeneuve d'Ascq Cédex, France*

We investigate the existence of defect modes in the photonic band structure of a comblike waveguide geometry made of dangling side branches grafted periodically along an infinite monomode waveguide. This one-dimensional photonic crystal exhibits forbidden bands that originate both from the periodicity of the system and the resonance states of the grafted branches. The defect modes result from the presence of defective branches in the comb and may occur in these stop bands. The localized states appear as very narrow peaks in the transmission spectrum of finite comblike waveguides composed of a finite number of grafted branches. The behavior of the localized states is analyzed as a function of the length, of the position, and of the number of the defective branches. These theoretical results are confirmed by experiments using coaxial cables in the frequency range of a few hundreds of MHz. [S0163-1829(99)04519-1]

I. INTRODUCTION

For the last ten years, numerous theoretical and experimental investigations have focused on the existence of gaps in the electromagnetic band structure of the *photonic crystals*, i.e., artificial structures exhibiting a spatially dependent dielectric constant. Various one-dimensional (1D), 2D, and 3D structures of periodic photonic crystals were studied.[1] Gaps were also observed in slightly disordered[2,3] as well as in quasiperiodic[4] 2D photonic crystals. In these forbidden bands, electromagnetic modes, spontaneous emission, and zero-point fluctuations are all absent.[5] These properties become more pronounced when the band gap is made large. Some studies have also addressed the problem of the emergence of localized states in the photonic band gaps (PBG) by introducing defects in the periodic dielectric structure. In 1D photonic crystals, i.e., classic Bragg mirrors,[6,7] defects may be layers of different nature than the other slabs. In 2D and 3D photonic crystals made of a periodic distribution of dielectric cylindrical or spherical inclusions embedded in a dielectric matrix, defect modes were observed by removing or adding some inclusions[8–10] or by changing the characteristics (material or diameter) of several inclusions.[11] These properties started also to be investigated in quasi-one-dimensional photonic crystals.[12] Photonic crystals possessing localized modes in the forbidden bands should have several applications to optical devices such as selective frequency filters or very efficient waveguides.

In two previous papers,[13,14] we proposed a model of a one-dimensional photonic crystal exhibiting very narrow pass bands separated by large forbidden bands. This system is composed of an infinite one-dimensional waveguide (*the backbone*) along which stars of N' finite side branches are grafted at N equidistant sites, N and N' being integers (see Fig. 1). This *star waveguide* is described by two structural and two compositional parameters, namely the periodicity

d_1, the length d_2 of each side branch and the relative dielectric permittivity ε_i of each medium with $i=1$ for the backbone and $i=2$ for the side branches. The one-dimensional nature of the model requires that the lengths d_1 and d_2 must be very much greater than the diameter of the backbone and the side branches. This retains its validity to monomode propagation of electromagnetic waves. The stop bands originate both from the periodicity of the system and the resonance states of the grafted branches, which play the role of resonators. Wide gaps/narrow bands can be obtained by an appropriate choice of the parameters, in particular the ratio between the two characteristic lengths d_1 and d_2. Moreover, by increasing the number N' of side branches grafted on each node, the forbidden bands can be strongly enlarged. Let us stress that, unlike in the usual photonic crystals,[1] relatively large gaps still remain for homogeneous systems where the branches and the backbone are constituted of the same material. We also proposed another way of making very large stop bands,[15] i.e., a tandem structure composed of two or several succesive comblike waveguides, which differ by their physical characteristics. Very large gaps in this system result from the superposition of the band gaps in the individual combs.

In this paper, we focus on the existence of localized modes inside gaps when defective branches of different length and constituted of a different material are inserted in
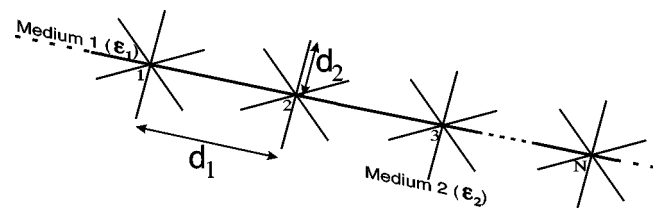
FIG. 1. Periodic waveguide with N stars of N' ($N'=6$, here) grafted branches.

the star waveguide. We show that the localized states appear as very narrow peaks in the transmission spectrum of comblike waveguides composed of a finite number of grafted branches. We analyze the behavior of the localized states as a function of the length, of the position, and of the number of the defective branches. The theoretical results are confirmed by experiments using coaxial cables in the frequency range of a few hundreds of MHz.

This paper is organized as follows. In Sec. II, we give the analytic expressions for the band structure of the periodic star waveguide and for the transmission coefficient through a finite comb with and without defects. Section III is devoted to a numerical discussion of these expressions as well as to a comparison of the theoretical results with experimental measurements. Finally, conclusions of this work are reported in Sec. IV.

II. MODEL

The pass and stop bands of the star waveguide depicted in Fig. 1 can be displayed in the dispersion relation for an infinite number of sites ($N \rightarrow \infty$) or in the transmission coefficient T through the waveguide when the side branches are grafted at a finite number N of nodes. Both the dispersion relation and the transmission factor T were obtained in a closed form by using the "interface response theory" (IRT).[13,16] They are given as

$$\cos(kd_1) = C_1 + \frac{N'}{2} \frac{F_2}{F_1} \frac{S_1 C_2}{S_2} \qquad (1)$$

or

$$\cos(kd_1) = C_1 + \frac{N'}{2} \frac{F_2}{F_1} \frac{S_1 S_2}{C_2} \qquad (2)$$

and

$$T = \left| \frac{2S_1(t^2-1)t^N}{A^2 - B^2 t^{2N}} \right|^2, \qquad (3)$$

where k is the modulus of the wave vector for propagation of electromagnetic waves in the star waveguide and $t = \exp(jkd_1)$. In Eqs. (1) and (2), the quantities C_i, S_i, and F_i ($i = 1,2$) are defined as $C_i = \cosh(\alpha_i d_i)$, $S_i = \sinh(\alpha_i d_i)$, and $F_i = \alpha_i$ with $\alpha_i = j\omega \sqrt{\varepsilon_i}/c$ where ω is the wave circular frequency, c the speed of light in vacuum, and $j = \sqrt{-1}$. The dispersion relations (1) and (2) were obtained for two different choices of the boundary conditions, namely, the vanishing of either the electric field ($E = 0$) or the magnetic field ($H = 0$) at the free extremities of the side branches. The modulus of the wave vector k is then given by either Eqs. (1) or (2). In Eq. (3), A and B are defined as

$$A = 1 - t(C_1 - S_1) \qquad (4)$$

and

$$B = t - (C_1 - S_1). \qquad (5)$$

On the other hand, the localized states in the band structure are obtained by removing, on one site of the photonic crystal depicted in Fig. 1, N_2' resonators and replacing them by N_3'

branches of length d_3 ($\neq d_2$), constituted of a material of relative dielectric permittivity ε_3 ($\neq \varepsilon_2$). Using the IRT, one can calculate analytically the frequencies of the localized states in the case of an infinite comb, i.e., with an infinite number of nodes ($N \rightarrow \infty$). They are given by the relation

$$1 + \chi \frac{t}{t^2 - 1} = 0. \qquad (6)$$

In the latter equation, the parameter χ characterizes the perturbation introduced in the comb by the defective resonators and is defined as

$$\chi = \frac{S_1}{F_1} \left(N_2' \frac{F_2 C_2}{S_2} - N_3' \frac{F_3 C_3}{S_3} \right) \qquad (7)$$

when the electric field $E = 0$ vanishes at the free ends of all the resonators and as

$$\chi = \frac{S_1}{F_1} \left(N_2' \frac{F_2 S_2}{C_2} - N_3' \frac{F_3 S_3}{C_3} \right) \qquad (8)$$

when the boundary condition $H = 0$ has been taken into account. In Eqs. (7) and (8), the symbols F_3, C_3, and S_3 associated with the defects have the same meaning as above. The transmission coefficient through a defective star waveguide with a finite number N of nodes can be obtained as

$$T = \left| \frac{2S_1(t^2-1)^2 t^N}{(A^2 - B^2 t^{2N})(t^2-1) + \chi \psi} \right|^2, \qquad (9)$$

where

$$\psi = \{ t(A^2 + B^2 t^{2N}) - AB[t^{2(N-n+1)} + t^{2n}] \}. \qquad (10)$$

In Eq. (10), the integer n, such as $1 \leq n \leq N$, stands for the location of the defects in the finite comb. One can easily check that for $\chi = 0$ (i.e., $N_2' = N_3' = 0$), which corresponds to the comb without defect, Eq. (10) leads to Eq. (3). One can also readily verify that the same transmission coefficient is obtained for two symmetrical locations of the defects with respect to the middle of the comb.

III. APPLICATIONS

In this section, we shall numerically illustrate the above analytic results for comblike waveguides composed of identical constituents, i.e., $\varepsilon_1 = \varepsilon_2$, with the same characteristics lengths $d_1 = d_2$ and the boundary condition $E = 0$. In Fig. 2, we present the band structures and transmission coefficients of the waveguide with and without defects. The top and bottom panels, respectively, describe the situations where the number of grafted side branches at every node is $N' = 1$ and $N' = 4$. Figure 2(a) shows the six lowest dispersion curves of the photonic band structure for $N \rightarrow \infty$ and $N' = 1$. The plots are given in terms of the reduced frequency $\Omega = \omega d_1 \sqrt{\varepsilon_1}/c$ versus the reduced wave vector kd_1. In this perfectly periodic system, one notes the presence of pass bands separated by gaps and in particular the existence of a cutoff frequency, i.e., a forbidden band that commences at zero frequency. The flat bands at reduced frequencies equal to $\pi, 2\pi, 3\pi, \ldots$ correspond to modes whose eigenfunctions vanish at every
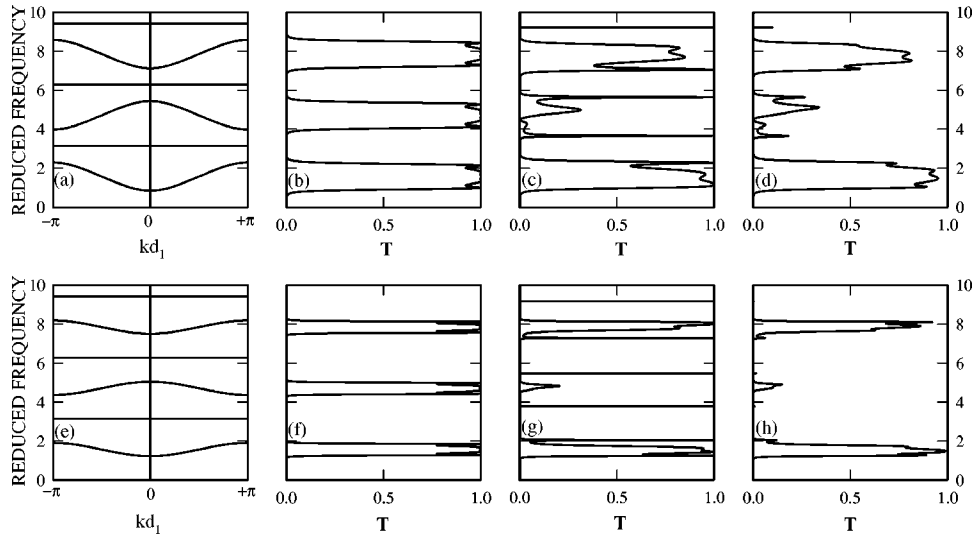
FIG. 2. *Top panel*: (a) Dispersion curves for the one-dimensional structure depicted in Fig. 1, with $N \to \infty$, $N' = 1$ and the boundary condition $E = 0$. The other parameters are $d_1 = d_2$ and $\varepsilon_1 = \varepsilon_2$. (b) Transmission coefficient through the same structure with the side branches grafted at $N = 5$ nodes. (c) Transmission coefficient through a comb containing one defect of length $d_3 = 0.7d_1$ ($\varepsilon_3 = \varepsilon_1 = \varepsilon_2$) located on the middle node ($N_2' = 1$ and $N_3' = 1$). The other parameters are the same as in (b). (d) Transmission coefficient through the same comb as in (c) but the defect is located on the second or on the fourth node. *Bottom panel*: Same as in top panel, but for $N' = 4$ side branches grafted at every node. In (g) [respectively (h)], $N_2' = 4$ resonators grafted at the middle (respectively second or fourth) node have been replaced by $N_3' = 1$ defective branch ($d_3 = 0.7d_1$ $\varepsilon_3 = \varepsilon_1$).

node of the comb structure. This means that these modes are eigenfunctions of the independent chains, constituting both the resonators and the backbone, without any interaction between the different chains. In Fig. 2(b), we have plotted the variations of the transmission coefficient T versus the reduced frequency for a finite number of nodes, namely $N = 5$. Despite the finite number of resonators, one can notice that T approaches zero in regions corresponding to the observed gaps in the electromagnetic band structure of Fig. 2(a). The flat bands in Fig. 2(a) do not contribute to the transmission since the corresponding eigenfunctions vanish at every node of the comb structure. We have shown[13,14] that increasing the number N of nodes to 10 and more, does not modify significantly the edges of the forbidden bands. In Fig. 2(c), the resonator located at the middle node, namely $N = 3$, has been replaced by a defective branch of length $d_3 = 0.7d_1$ and of relative dielectric constant $\varepsilon_3 = \varepsilon_1$. In the frequency range displayed in Fig. 2(c), there are five peaks associated with the localized states; those falling in the middle of a gap being much narrower than those situated in the vicinity of a band edge. The transmission inside a pass band is also significantly affected by the presence of the defect as can be observed in the second pass band of Fig. 2(c) where T is totally depressed. Figure 2(d), where the defect is located on the second or on the fourth node, highlights the influence of the location of the defect site on the transmission coefficient and in particular on the intensities of the peaks associated with the localized modes. The bottom panel of Fig. 2 contains similar results to those of the top panel when several ($N' = 4$) side branches are grafted at every node. This panel illustrates the narrowing (widening) of the pass bands (forbidden bands) when increasing N'. Figure 2(g) [respectively Fig. 2(h)] shows the variation of the transmission coefficient when the four resonators located on the middle (respectively second or fourth) node have been re-

placed by one defective branch ($d_3 = 0.7d_1$ and $\varepsilon_3 = \varepsilon_1$). In this case, some of the peaks associated with the defect modes are more clearly detached from the band edge, than in Fig. 2(c), especially those around the second pass band. One also observes that these peaks are much narrower in Fig. 2(g) than in Fig. 2(c). This is clearly illustrated in Fig. 3 where the peaks appearing around $\Omega \approx 9$ in Figs. 2(c) and 2(g) have been plotted on the same graph at the same scale. We have also investigated the influence of the number of grafted defects on the localized modes. The top panel of Fig. 4 shows the variations of the transmission coefficient through a nondefective comb whose parameters are $N = 5$, $N' = 1$. The three other panels present the transmission when the resonator grafted on the middle node has been replaced by $N_3' = 1, 2,$ and 4 defective branches of length $d_3 = 0.7d_1$. The transmission factor in the pass bands is more and more depressed as N_3' increases. The localized states are getting closer to the middle of the gaps when increasing N_3'. These states become more and more confined, i.e., the quality factor of the peaks defined as the ratio between the central fre-
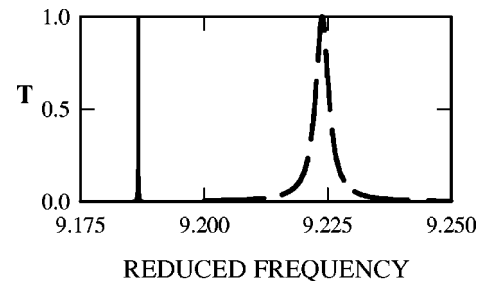
FIG. 3. Comparison between the shape of the peaks associated with the localized state appearing around $\Omega \approx 9$ in Figs. 2(c) (*dashed line*) and 2(g) (*solid line*). One observes that increasing N' produces a decrease in the width of the peak.
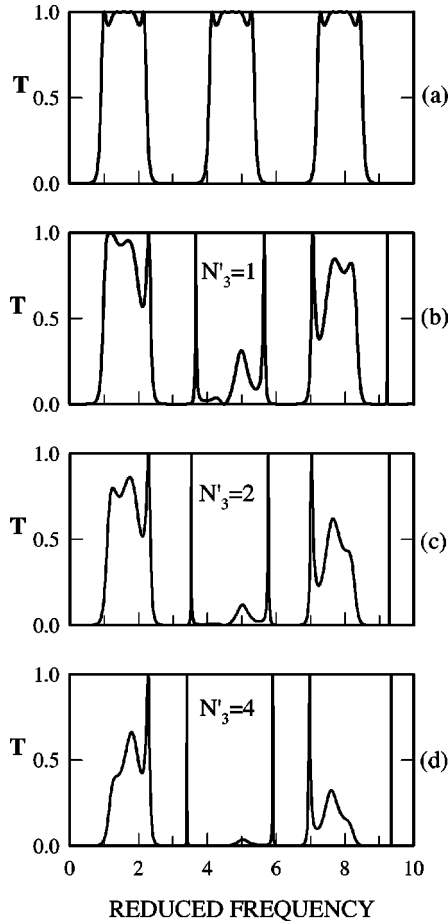
FIG. 4. Transmission coefficients versus the reduced frequency through four combs without defect [(a)] and with defects [(b), (c), and (d)]. The results are illustrated for $N=5$, $N'=1$, $\varepsilon_1 = \varepsilon_2$, $d_1 = d_2$ with the boundary condition $E=0$. In (b), (c), and (d), the resonator grafted at the middle node has been replaced by $N'_3 = 1$, 2, and 4 defective branches ($d_3 = 0.7d_1$ and $\varepsilon_1 = \varepsilon_3$).

quency and the full width at half maximum increases. Figure 5 focus on the peak associated with the localized state appearing around $\Omega \approx 9$ in Figs. 4(b), 4(c), and 4(d). This figure shows together the shifting in frequency of this peak as well as the increase of its quality factor with increasing N'_3. From Figs. 2, 4, and 5, one can conclude that an increase of N' or N'_3 in the comb gives rise to narrower peaks.

In Fig. 6(a), we present the reduced frequencies of the localized modes as a function of the ratio d_3/d_1 for a fixed
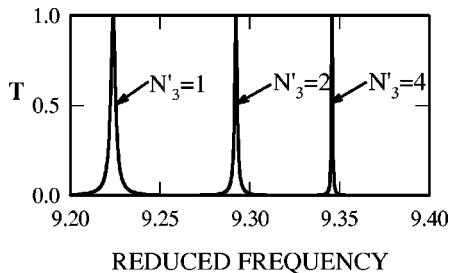
FIG. 5. The shape of the peak associated with the localized state appearing in Figs. 4(b), 4(c), and 4(d) around $\Omega \approx 9$ is illustrated at a larger scale to show the increase in the quality factor with increasing N'_3.

value of ε_3 when one resonator in an infinite comb has been replaced by one defective branch. The hatched areas correspond to the pass bands of the perfect comb with $N'=1$. One observes that the localized modes emerge from the pass bands, decrease in frequency by increasing d_3 and finally merge into a lower pass band. At each frequency, there is a periodical repetition of the localized state as a function of d_3. The same observations may be done in Fig. 6(b) where the length d_3 of the defect has been fixed and its relative dielectric constant ε_3 varies. These figures clearly show that the frequencies of the localized states inside the forbidden bands strongly depend on the physical characteristics of the defective side branch. For example, one observes in Fig. 6(a) that the localized states occur in the middle of the second forbidden band for $d_3/d_1 \approx 0.5, 1, 1.5 \ldots$. Figures 6(c) and 6(d) present similar results for an infinite comb with $N'=4$ and the same other parameters. The defect modes were obtained by replacing four resonators in one node by a defective branch of length d_3 or made of a material of relative dielectric constant ε_3.

The results presented in this paper were obtained with the boundary condition $E=0$ at the free ends of the resonators. Qualitatively similar results are also obtained by using the boundary condition $H=0$ at the free extremities of the side branches, although the gaps are narrower in this case with our choice of $d_1 = d_2$ and $\varepsilon_1 = \varepsilon_2$.[13,14]

In order to check the validity of the above theoretical predictions in a frequency range up to 500 MHz, we have performed experiments where both the one-dimensional waveguide and the side branches are constituted by standard 50Ω coaxial cables. The transmission measurements have been realized by using a tracking generator coupled to a spectrum analyzer. We have compared the experimental measurements with the theoretical predictions for combs without and with defects. As predicted by the theoretical results, an increase of N' or N'_3 in the comb, gives rise to a narrowing of the peaks associated with the localized states. For comb-like waveguides with N' and $N'_3 \geqslant 4$, the resolution of our experimental setup does not allow to detect these very sharp peaks. Then we limited ourself to study experimentally the propagation of electromagnetic waves in defective combs with N' and $N'_3 \leqslant 2$. The upper panel of Fig. 7 shows the theoretical and experimental variations of the transmission coefficient through a perfect comb whose parameters are $N=5$, $N'=1$, $\varepsilon_1 = \varepsilon_2 = 2.3$, and $d_1 = d_2 = 1m$; the boundary condition being $E=0$ at the free ends of the grafted resonators. The width and the frequency domains of the pass and stop bands are quite similar in both spectra. The attenuation of the amplitude in the experimental signal with growing frequency, observed in Fig. 7(b), is well-known in this kind of coaxial cables. The variations of T when the coaxial cable of length $d_2 = 1m$ grafted on the middle node is replaced by an other cable of length $d_3 = 1.175m$ are presented in the middle panel. The localized modes appear in the experimental spectrum as peaks whose frequencies agree quite well with the theoretical prediction. The widening of these peaks with growing frequency is also observed in both spectra. Because of the resolution of the experimental setup, the amplitude of the peaks appears weaker in the experimental spectrum than in the theoretical spectrum. The presence
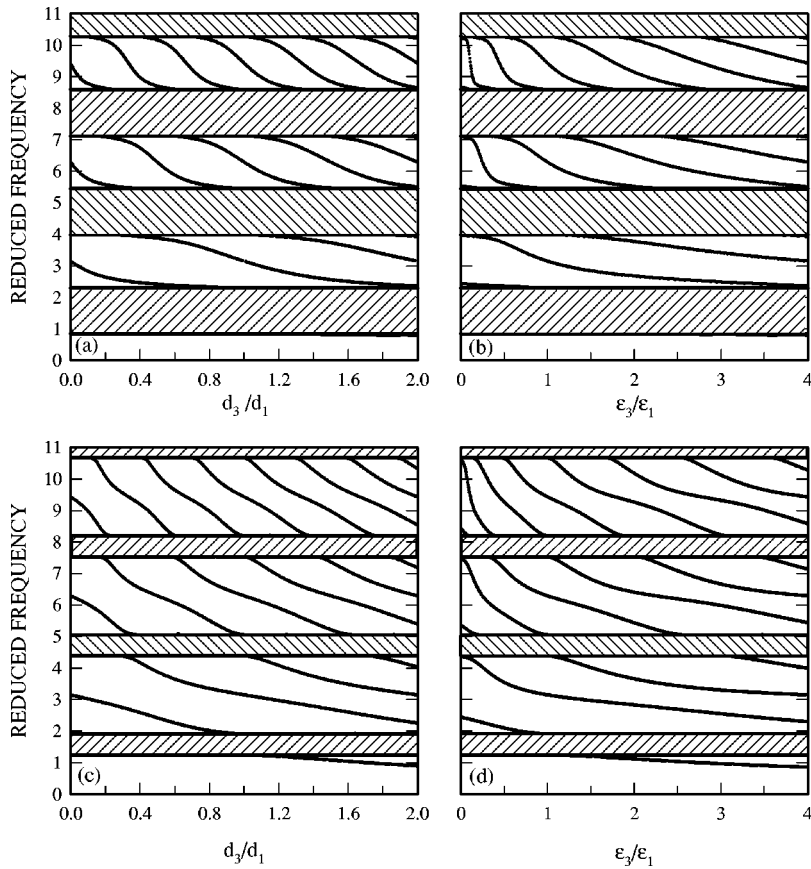
FIG. 6. *Top Panel*: Reduced frequencies of the localized modes associated with $N'_3 = 1$ defective side branch inserted in an infinite comb ($N \to \infty$). The characteristics of the comb are $N' = 1$, $\varepsilon_1 = \varepsilon_2$, $d_1 = d_2$ and the boundary condition is $E = 0$. (a) The length d_3 of the defective branch varies and its relative dielectric permittivity ε_3 is fixed and equal to ε_1. (b) The relative dielectric permittivity ε_3 of the defective branch varies and its length d_3 is fixed and equal to d_1. *Bottom Panel*: Same as in top panel, but for $N' = 4$ side branches grafted at every node. In (c) and (d), $N'_2 = 4$ resonators grafted at one node of the infinite comb have been replaced by $N'_3 = 1$ defective branch (d_3, ε_3).
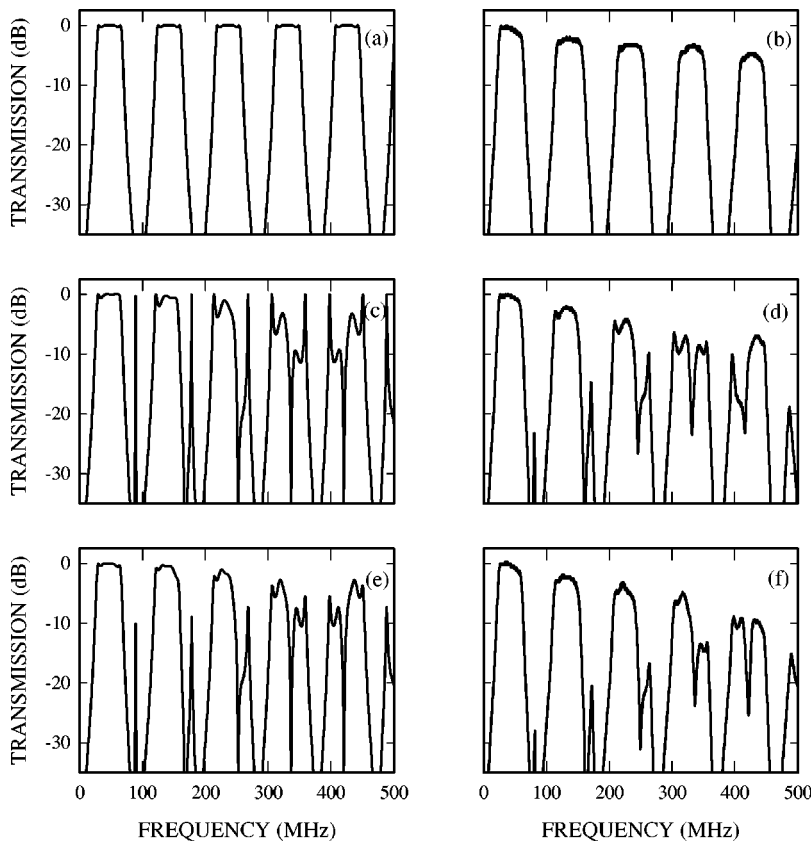
FIG. 7. Comparison between the theoretical [(a), (c), and (e)] and experimental [(b), (d), and (f)] transmission coefficients through (a) and (b): a perfect comb of characteristics $N = 5$, $N' = 1$, $\varepsilon_1 = \varepsilon_2 = 2.3$, $d_2 = d_1 = 1m$ with the boundary condition $E = 0$ ($N'_2 = N'_3 = 1$). (c) and (d): the same comb containing one defect of length $d_3 = 1.175m$ ($\varepsilon_3 = \varepsilon_1 = 2.3$) located on the middle node. (e) and (f): the same comb but with the defect located on the fourth node.
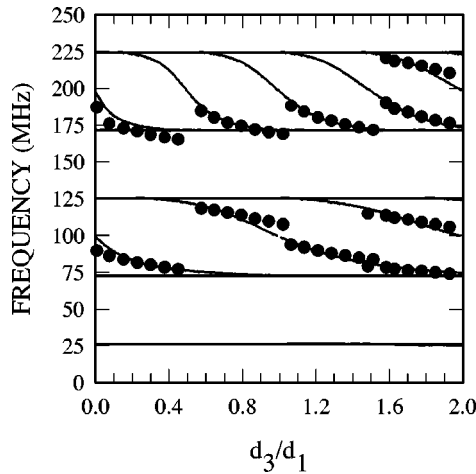
FIG. 8. Comparison between the theoretical and the experimental frequencies of the localized states associated with the presence of a defect of length d_3 in a comb ($N_2' = N_3' = 1$) *thin line*: calculated frequencies in an infinite comb ($N \to \infty$). *filled dots*: measured frequencies in a finite comb with $N = 5$. The other parameters are $N' = 1$, $d_1 = d_2 = 1m$, $\varepsilon_1 = \varepsilon_2 = \varepsilon_3 = 2.3$ and the boundary condition is $E = 0$. The flat lines correspond to the edges of the pass-bands.

of the defective branch also affects the transmission in the third, fourth and fifth pass bands. Finally the bottom panel shows the behavior of T when the same defect branch is located on the fourth node. This behavior is similar to the previous one except for the strongest attenuation of the transmission in the fourth and fifth passbands as well as the weaker amplitude of the peaks associated with the localized states.

Other experiments have been performed on the above-described comb structure with one *defect* coaxial cable grafted on the middle node. Transmission has been measured for various values of d_3. The frequencies of the localized states associated with the defective resonator were measured using the spectrum analyzer. For each value of d_3, we have compared the experimental frequencies measured on a finite comb with the theoretical frequencies calculated on the *equivalent* infinite comb. The results are displayed in Fig. 8. The theoretical and experimental values are in reasonable agreement. The shift in frequency observed for a few points may be attributed to the finite number of resonators taken into account in the experimental setup. We have obtained

similar results with star waveguides possessing two grafted resonators at each node. The forbidden bands are slightly wider in this case.

IV. CONCLUSION

We have investigated the propagation of electromagnetic waves in comblike structures composed of multiple dangling side branches grafted on an infinite waveguide. The theoretical model assumed that the cross sections of the waveguide and of the side branches are small compared to their linear dimensions, that is, they may be considered as one-dimensional media. This retains the validity of the model to monomode propagation of electromagnetic waves. These comblike structures may present large stop bands and are good candidates for PBG materials. We have shown that the presence of defective branches in the comb gives rise to localized states inside the forbidden bands. These defect modes appear as very narrow peaks of strong amplitude in the transmission spectrum. The localized states are very sensitive to the length of the defects, to their location in the comb as well as to their number. Experimental measurements using coaxial cables have confirmed the theoretical predictions for frequencies up to 500 MHz. However, our theoretical model is, in principle, universal and then also valid in other frequency domains of the electromagnetic spectrum. Indeed, the frequency domains where the PBG occur only depends on the periodicity of the comblike structure and the length of the grafted branches. The manufacturing of such waveguides could be very usefull in making, for instance, filtering, or multiplexing devices. It would even be more interesting for integrated structures working at optical frequencies. One must observe that for optical frequencies, the periodicity and the length of the side branches must be of the order of magnitude of the micrometer. Recents works show clearly that the manufacturing of such comblike structures at a submicrometric scale becomes realizable with the new technological developments using high-resolution electron beam lithography.[12,17]

*Author to whom correspondence should be addressed.

[1] See, for example, J. D. Joannopoulos, R. D. Meade, and J. N. Winn, *Photonic Crystals* (Princeton University Press, Princeton, 1995); *Photonic Band Gaps and Localization*, edited by C. M. Soukoulis (Plenum, New York, 1993); *Photonic Band Gap Materials*, edited by C. M. Soukoulis (Kluwer, Dordrecht, 1996).

[2] M. M. Sigalas, C. M. Soukoulis, C. T. Chan, and D. Turner, Phys. Rev. B **53**, 8340 (1996).

[3] H. Li, B. Cheng, and D. Zhang, Phys. Rev. B **56**, 10 734 (1997).

[4] Y. S. Chan, C. T. Chan, and Z. Y. Liu, Phys. Rev. Lett. **80**, 956 (1998).

[5] E. Yablonovitch, J. Opt. Soc. Am. B **10**, 283 (1993).

[6] R. P. Stanley, R. Houdré, U. Oesterle, M. Ilegems, and C. Weisbuch, Phys. Rev. A **48**, 2246 (1993).

[7] R. Wang, J. Dong, and D. Y. Xing, Phys. Status Solidi B **200**, 529 (1997).

[8] M. Sigalas, C. M. Soukoulis, E. N. Economou, C. T. Chan, and K. M. Ho, Phys. Rev. B **48**, 14 121 (1993).

[9] E. Yablonovitch, T. J. Gmitter, R. D. Meade, A. M. Rappe, K. D. Brommer, and J. D. Joannopoulos, Phys. Rev. Lett. **67**, 3380 (1991).

[10] A. Mekis, J. C. Chen, I. Kurland, S. Fan, P. R. Villeneuve, and J. D. Joannopoulos, Phys. Rev. Lett. **77**, 3787 (1996).

[11] K. Sakoda and H. Shiroma, Phys. Rev. B **56**, 4830 (1997).

[12] S. Foresi, P. R. Villeneuve, J. Ferrera, E. R. Thoen, G. Steinmeyer, S. Fan, J. D. Joannopoulos, L. C. Kimerling, H. I. Smith, and E. P. Ippen, Nature (London) **390**, 143 (1997).

[13] J. O. Vasseur, P. A. Deymier, L. Dobrzynski, B. Djafari Rouhani, and A. Akjouj, Phys. Rev. B **55**, 10 434 (1997).

[14] L. Dobrzynski, A. Akjouj, B. Djafari Rouhani, J. O. Vasseur, and J. Zemmouri, Phys. Rev. B **57**, R9388 (1998).

[15] B. Djafari Rouhani, J. O. Vasseur, A. Akjouj, L. Dobrzynski, M. S. Kushwaha, P. A. Deymier, and J. Zemmouri, Prog. Surf. Sci. **59**, 255 (1998).

[16] L. Dobrzynski, Surf. Sci. **180**, 489 (1987).

[17] G. Feiertag, W. Ehrfeld, H. Freimuth, H. Kolle, H. Lehr, M. Schmidt, M. M. Sigalas, C. M. Soukoulis, G. Kiriakidis, T. Pedersen, J. Kuhl, and W. Koenig, Appl. Phys. Lett. **71**, 1441 (1997).